

# Directional Couplers Using Long-Range Surface Plasmon Polariton Waveguides

Alexandra Boltasseva and Sergey I. Bozhevolnyi

(Invited Paper)

**Abstract**—We present an experimental study of guiding and routing of electromagnetic radiation along the nanometer-thin and micrometer-wide gold stripes embedded in a polymer via excitation of long-range surface plasmon polaritons (LR-SPPs) in a very broad wavelength range from 1000 to 1650 nm. For straight 14-nm-thick stripes and a wavelength of 1550 nm, LR-SPP propagation loss is determined for the stripe widths varying from 2 to 12  $\mu\text{m}$  and is found to be  $\sim 7$  and 5 dB/cm for 10- and 4- $\mu\text{m}$ -wide stripes, respectively. For the directional couplers based on 14-nm-thick and 8- $\mu\text{m}$ -wide gold stripes and a wavelength of 1570 nm, the coupling lengths of 4.1, 1.9, and 0.8 mm are found for the respective waveguide separations of 8, 4, and 0  $\mu\text{m}$ . We model the LR-SPP-based directional couplers using the effective-refractive-index method and obtain a good agreement with the experimental results. The transmission spectra of LR-SPP-based directional couplers are presented demonstrating an efficient ( $\sim 30$  dB) separation of different telecom wavelength bands. Various possibilities for dynamic control of wavelength division/multiplexing with LR-SPP-based directional couplers that utilize the thermo-optic effect in the polymer cladding are also discussed.

**Index Terms**—Directional couplers, integrated optics, surface waves, waveguide components.

## I. INTRODUCTION

IN recent years, optics of surface plasmon polaritons (SPPs) [1] have attracted much interest in the context of highly integrated photonic devices and nano-optics [2]. SPPs represent quasi-two-dimensional (2-D) electromagnetic (EM) excitations propagating along a dielectric–metal interface having the EM field amplitudes strongly enhanced at the interface and decaying exponentially into both the neighboring media [1]. Rather tight field intensity confinement to the metal surface (typically of the order of or smaller than the wavelength in the corresponding media) makes SPPs very sensitive to surface irregularities, which enables their use in surface analysis, including biosensing. The same feature allows one to manipulate the SPP in the surface plane by using different types of surface metal nanostructures. With the recent progress in nanofabrication, efficient control of SPP propagation has been achieved in the different scattering and guiding surface configurations [1]–[7]. However, a limita-

Manuscript received December 14, 2005; revised June 8, 2006. This work was supported by the Danish Technical Research Council under Contract 26-03-0158. The work of A. Boltasseva was supported by the Danish Technical Research Council under “Talent Project” Grant 26-04-0268.

A. Boltasseva is with the Department of Communications, Optics and Materials and Centre for Nanotechnology, Technical University of Denmark, Lyngby DK-2800, Denmark (e-mail: aeb@com.dtu.dk).

S. I. Bozhevolnyi is with the Department of Physics and Nanotechnology, Aalborg University, Aalborg DK-9220, Denmark.

Digital Object Identifier 10.1109/JSTQE.2006.882659

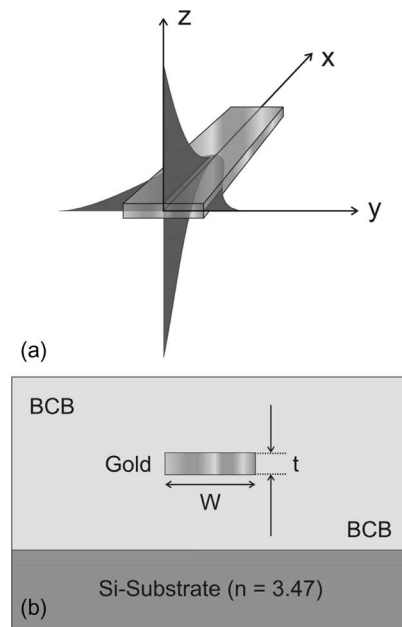


Fig. 1. (a) Schematic of the LR-SPP mode field distribution in transverse ( $z$ ) and lateral ( $y$ ) directions. (b) Schematic of the sample geometry: Metal stripe of thickness  $t$  and width  $w$  surrounded by BCB polymer layers. The structure is placed on a silicon substrate.

tion to the use of SPPs in optical devices is its low propagation length at optical frequencies ( $\sim 30 \mu\text{m}$  in visible and  $\sim 300 \mu\text{m}$  in near-infrared, for a silver–air interface) and the difficulty of efficiently coupling light in and out of the structure.

These restrictions to the applicability of SPP devices have led to explorations of another avenue of SPP research that focuses on a special SPP subset, namely long-range surface plasmon polaritons (LR-SPPs) [8] propagating on nanometer-thin metal films or stripes embedded in a dielectric material [Fig. 1(a)]. Propagation of LR-SPP modes was first considered for thin, infinitely wide metal films [8], [9] and later for metal films of finite width [10]. Such symmetrical structure supports the propagation of the field-symmetrical modal solution, whereby a coupling of SPPs at two metal–dielectric interfaces results in a very small field concentration within the central metal film, and hence, a low propagation loss for the LR-SPP. At the same time, for sufficiently thin metal films, the LR-SPP field components extend over several micrometers into the cladding via two identical evanescent tails facilitating the optical excitation, because the mode size is now close to that of the standard single-mode (SM) fiber [Fig. 1(a)]. The end-fire excitation of LR-SPPs was first proposed by Burke *et al.* [9] and realized by Charbonneau

*et al.* [11] who experimentally observed the LR-SPP propagation along thin gold stripes of finite width embedded in silica glass. Later, efficient LR-SPP excitation and guiding (at telecommunication wavelengths) along thin gold stripes embedded in a dielectric was realized demonstrating a coupling loss of  $\sim 0.5$  dB and propagation loss of  $\sim 6$ – $8$  dB/cm for benzocyclobutene-gold-benzocyclobutene (BCB–Au–BCB) configuration [12] and propagation loss as low as 4.2 dB/cm combined with 98% excitation efficiency for polymer-Au-glass configuration [13].

Low propagation and coupling loss attainable with LR-SPPs have stimulated the experimental studies of LR-SPP-based integrated optics (IO), and different passive components including straight and bent waveguides, Y-splitters, multimode interference devices, and directional couplers (DCs) have been recently demonstrated [14], [15]. As an alternative approach for making IO circuits, LR-SPP stripe waveguides have one unique feature—the possibility of using the same metal-stripe circuitry for both guiding optical radiation and transmitting electrical signals that control its guidance. Lately, efficient LR-SPP-based dynamic devices with low power consumption, including various modulators and switches, have been also realized utilizing the thermo-optic effect in the polymer cladding [16], [17]. Moreover, together with different passive and active LR-SPP-based components for IO, two different approaches for making Bragg gratings based on LR-SPP-supporting configurations (by varying widths [18] and thickness [19] of the metal stripe) have been recently reported, where a very broad range of LR-SPP-based grating performance (from weak narrow-band gratings up to very strong and broadband gratings) has been experimentally demonstrated. LR-SPP-based components thereby constitute a promising alternative for the IO circuits meeting low-cost, simplicity of fabrication, flexibility, as well as performance requirements.

In this paper, we conduct further investigations of LR-SPP-based waveguide components and report in detail on the performance of polymer-based LR-SPP stripe waveguides and DCs. In a very broad wavelength range (1000–1650 nm), we investigate the guiding and routing of light along the thin gold stripes embedded in a polymer via excitation of LR-SPPs for different widths of stripe waveguides and DC parameters. The paper is organized as follows. In Section II, the fabrication procedure for making gold stripe waveguides is described together with the parameters of fabricated structures. Section III reports the experimental arrangement used for the optical characterization of waveguide components. Section IV is devoted to the experimental results obtained with the LR-SPP straight waveguides. Experimental values for the propagation and coupling losses for different waveguide widths are presented in the wavelength range from 1000 to 1650 nm, along with the calculated values for the propagation loss for one of the waveguide dimensions. In Section V, the performance of DCs based on LR-SPP stripe waveguides is demonstrated for different stripe widths and separations. Experimental values of the coupling lengths are then compared with the values calculated using the effective-refractive-index method. Section VI presents the transmission spectra of LR-SPP-based DCs exhibiting the efficient separation of different telecom

wavelength bands. The possibilities for the dynamic control of wavelength division/multiplexing with LR-SPP-based DCs that utilize the thermo-optic effect in the polymer are also discussed. Finally, the conclusion is presented in Section VII.

## II. FABRICATION

To fabricate the LR-SPP stripe waveguides [Fig. 1(b)], a silicon wafer was first spin-coated with a 15- $\mu\text{m}$ -thick layer of BCB (Cyclotene 3022-57, DOW Chemical Company), and then with a layer of ultraviolet (UV) resist. Straight stripes and directional couplers were patterned using standard UV lithography and fabricated by the deposition of thermally evaporated gold layer (14 nm) and a subsequent lift-off process. As the final fabrication step, the waveguide components were covered by a second 15- $\mu\text{m}$ -thick layer of BCB. Since the symmetry of the structure is very important for the LR-SPP properties (propagation loss, mode field diameter), it was so carefully controlled that the cladding layers had the same refractive index and were thick enough to accommodate the EM field of the LR-SPP. This was guaranteed by applying the same polymer for the top and bottom claddings and using identical spinning and curing conditions. After the final polymer curing, the wafer was cut into individual samples containing different waveguide devices. For cutback measurements, the samples with straight stripe waveguides were cut to different lengths.

Fabricated samples included straight stripe waveguides of different widths (from 2 to 12  $\mu\text{m}$ ) and DCs with different interaction lengths (from 0.1 to 8 mm) and separation between waveguides (from 0 to 8  $\mu\text{m}$  edge-to-edge-separated waveguides). DCs were based on stripe waveguides of different widths (from 2 to 10  $\mu\text{m}$ ).

## III. EXPERIMENT

For optical characterization of straight waveguides and DCs, standard spectrally resolved transmission measurements were performed. In order to excite the LR-SPP mode, end-fire coupling of light was performed using a laser (1570 nm, NetTest tunic plus) or a super continuum white light source (KOHHERAS SuperK) through a polarizer, as a source. Light polarized perpendicular to the waveguide plane was launched into the LR-SPP waveguide via butt-coupling from a polarization-maintaining (PM) fiber (Crystal Fibre LMA-PM-9) with a mode field diameter (MFD) of 7.2  $\mu\text{m}$ . To ensure that the polarization of light was orthogonal to the waveguide layer, angular adjustments of the PM fiber were performed. As an out-coupling fiber, standard SM fiber was used. Sample facets were not polished after dicing but index-matching liquid was used between the output fiber and the sample to improve the coupling conditions. The output signal was detected by a power meter (for measurements performed with the laser) or optical spectrum analyzer (for broadband measurements). The adjustment of the in- and out-coupling fibers with respect to the stripe waveguide was accomplished by maximizing the amount of light transmitted through a waveguide (active alignment). We should mention that almost all light coupled from the input fiber to the cladding was stripped away before reaching the end facet of the sample,

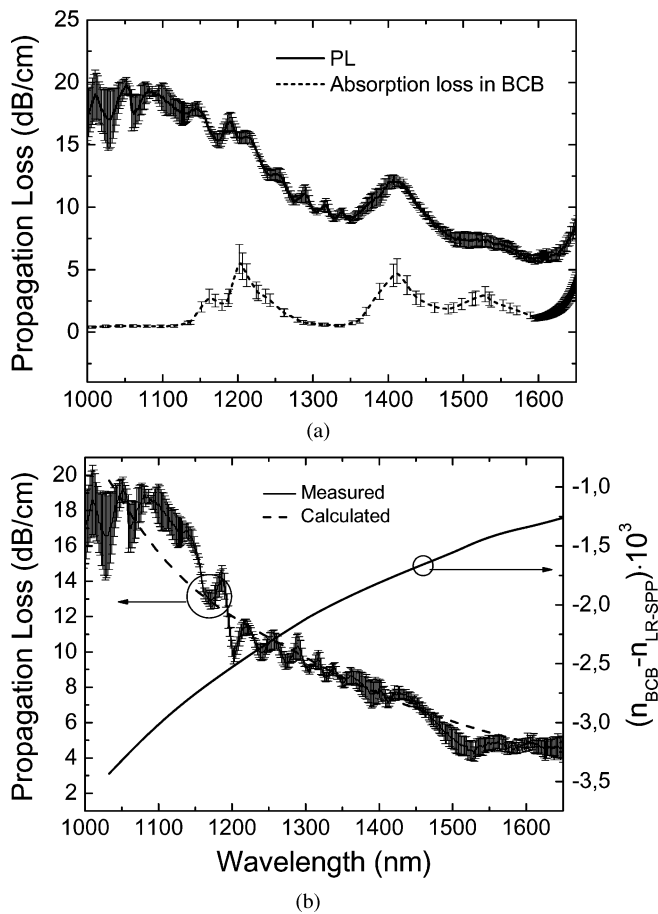


Fig. 2. Propagation loss (PL) measured for 10- $\mu\text{m}$ -wide and 14-nm-thick gold stripe waveguides. (a) Using cut-back method (together with absorption loss curve for BCB polymer). (b) After subtraction of BCB absorption loss (together with the calculated values of the propagation loss for infinite 14-nm-thick Au film performed using 1-D mode solver).

so that only the LR-SPP mode confined to a waveguide was observed at the output, making the alignments of the fibers quite easy. The output intensity distribution was monitored via an infrared Vidicon camera.

#### IV. STRAIGHT STRIPE WAVEGUIDES

The transmission measurements were performed for 14-nm-thick straight stripe waveguides of different widths from 2 to 12  $\mu\text{m}$ . At a particular wavelength, the propagation loss was found as the slope of the linear fit (cut-back method) to the experimental values of loss obtained for samples of different lengths (5, 10, 15, and 20 mm). This linear-fitting technique allowed estimating the coupling loss from the intersection point on the loss axis corresponding to the waveguide of zero length.

An example of the propagation loss dependence on the wavelength is shown in Fig. 2(a) for a 10- $\mu\text{m}$ -wide stripe waveguide. Propagation loss in a LR-SPP stripe waveguide has several contributions: the internal damping in metal (ohmic loss), scattering by inhomogeneities in the structure of a gold stripe (surface and edge roughness), and scattering and absorption in the polymer. It was previously shown that for thick metal stripes (more than 15 nm) the damping in metal is dominating [15], whereas for thin

metal stripes all loss contributions can be comparable. In order to eliminate the losses occurring in the polymer, the wavelength dependence of the absorption loss in BCB polymer [Fig. 2(a)] was extracted from the data provided by the DOW Chemical Company.<sup>1</sup> After the subtraction of the polymer absorption loss, the propagation loss in the stripe waveguide was compared with the values calculated using a one-dimensional (1-D) mode solver by Kymata Software [Fig. 2(b)]. The geometry considered in simulations consists of an infinite 14-nm-thick metal film surrounded by two identical dielectric layers characterized by the refractive index of the BCB polymer.<sup>1</sup> As in the real configuration, the structure was placed on a silicon substrate with a refractive index of 3.47. The metal in the analysis was gold with a complex refractive index [20]. Agreement between the experimental and calculated values of the propagation loss indicated that the internal damping in metal and polymer absorption were the dominating loss mechanisms in the investigated waveguides, whereas the contribution from the scattering loss in the polymer and in the waveguide was not large. It should also be emphasized that reasonable agreement between the experimental loss values and the calculated ones showed that the dielectric constant obtained for bulk gold [20] can be used in the modeling of investigated configurations involving nanometer-thick gold films. Note that, in similar investigations reported in [13], it was found that Au films less than 20 nm in thickness did not exhibit bulk properties and that the optical parameters of such a thin gold film were dependant on the thickness of the film. It seems reasonable to suggest that the minimal thickness, for which bulk-gold constant is still applicable, depends on the fabrication method and may vary for different metal deposition processes.

Together with the propagation loss, the effective refractive index of the LR-SPP mode was calculated using the above-mentioned mode solver. The difference between the refractive index of BCB and the effective refractive index of the LR-SPP, calculated for an infinitely wide 14-nm-thick Au film, is of the order of  $10^{-3}$  and decreases monotonically with the increase in the wavelength [Fig. 2(b)], which indicates that the fractional overlap of the LR-SPP mode with the metal decreases toward longer wavelengths. It should be noted that the effective refractive index for LR-SPP stripe modes is smaller than that plotted in Fig. 2(b) and can be estimated using the effective-index approach [15].

The coupling loss for waveguides of different widths is shown in Fig. 3(a) for the wavelength range from 1500 to 1650 nm. For stripe waveguides wider than 4  $\mu\text{m}$ , the coupling loss was found to be between 2 and 4 dB in the whole spectral range. The coupling loss value included in- and out-coupling losses from two different fibers: 1) PM fiber with nonwavelength-dependent MFD of approximately 7.2  $\mu\text{m}$  and 2) standard SM fiber with approximately 10  $\mu\text{m}$ -MFD at 1550 nm, which decreases with the wavelength. According to the modeling performed for an infinite 14-nm-thick gold film, the full-width at half-maximum (FWHM) of the transverse LR-SPP mode

<sup>1</sup>CYCLOTENE Advanced Electronics Resins: Refractive Index vs. Wavelength, The Dow Chemical Company, 2005. [Online]. Available: <http://www.dow.com/cyclotene/solution/refwave.htm>.

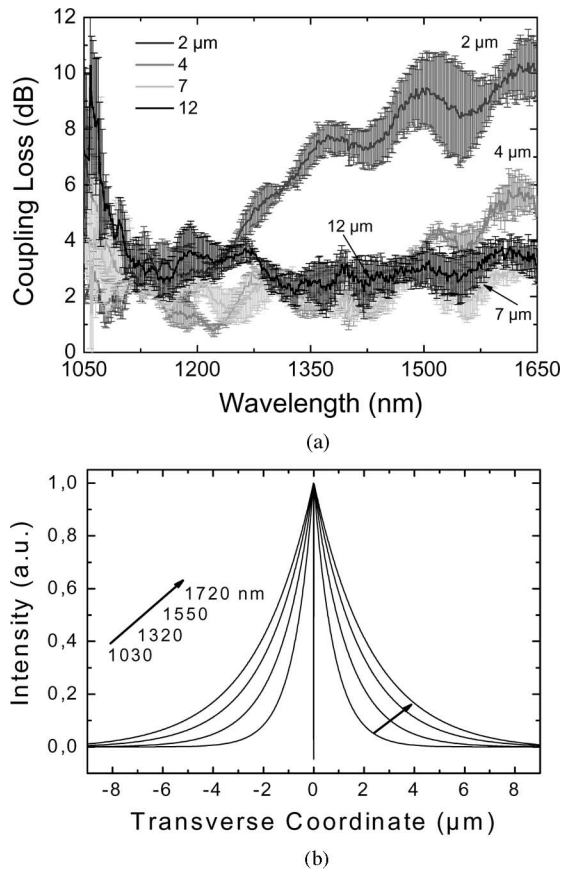


Fig. 3. (a) Coupling loss for stripe waveguides of different widths. (b) Transverse LR-SPP mode profiles for infinite 14-nm-thick Au film performed using 1-D mode solver.

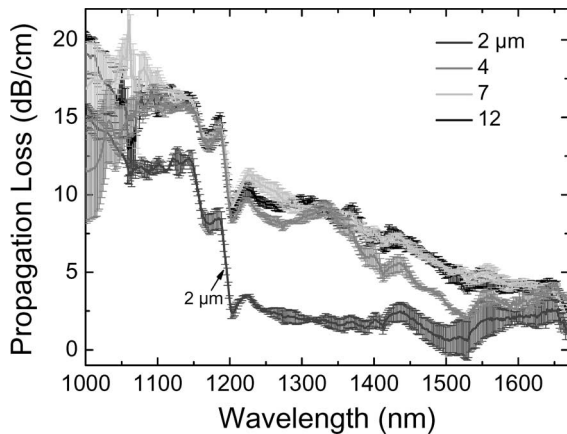


Fig. 4. Propagation loss (after subtraction of BCB loss) for stripe waveguides of different widths.

profile was decreasing with the wavelength from approximately 3.2  $\mu\text{m}$  at 1720 nm to 1.2  $\mu\text{m}$  at 1030 nm [Fig. 3(b)].

The propagation loss (with the polymer absorption loss subtracted) obtained for different waveguide widths is presented in Fig. 4. Propagation loss displayed a general tendency of decreasing with the reduction in waveguide width, a feature that was first theoretically predicted by Berini [10]. The decrease of the propagation loss with the stripe width implies the possibility of reaching very low propagation loss values at telecom wave-

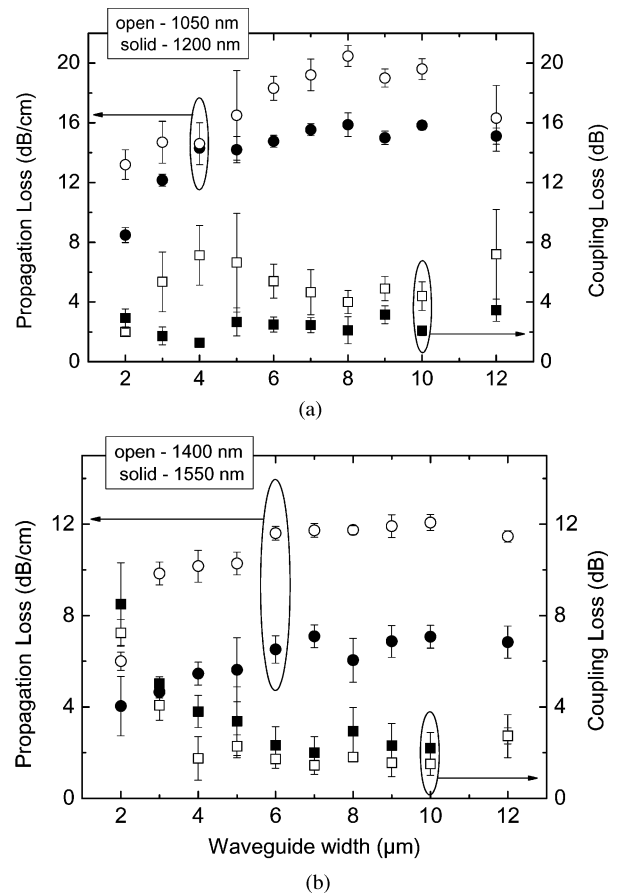


Fig. 5. Propagation and coupling losses dependences on the waveguide width. (a) 1050 nm (open symbols) and 1200 nm (solid symbols). (b) 1400 nm (open symbols) and 1550 nm (solid symbols).

lengths below 1 dB/cm for a 2- $\mu\text{m}$ -wide waveguide, and quite a reasonable loss level for the whole wavelength range from 1000 to 1650 nm when using low-loss dielectric cladding for gold stripes. For example, for a 2  $\mu\text{m}$ -wide stripe, the propagation loss was found to be below 3 dB/cm in the spectral range from 1200 to 1650 nm (Fig. 4).

Width dependence of the LR-SPP stripe waveguide performance is further demonstrated in Fig. 5, where the experimentally obtained propagation- and coupling-loss dependences on the stripe width are plotted for different wavelengths. There is always a tradeoff between the propagation and coupling loss, so that the decrease in propagation loss is accompanied by the increase in the coupling loss and vice versa. For example, at 1550 nm, the propagation loss can be decreased from 7.1 to 5.4 dB/cm simply by reducing the stripe width from 10 to 4  $\mu\text{m}$ , however, simultaneously increasing the coupling loss from 2.2 to 3.8 dB. This is due to the fact that the LR-SPP characteristics depend on the field localization. Weaker LR-SPP mode confinement (less field inside the metal stripe) observed for narrower stripes results in lower propagation loss but, at the same time, it becomes less bound to the metal stripe and extends more into the dielectric [12], [15] leading to a larger coupling loss. This also means that for a specific application in the given in- and out-coupling conditions, it is possible to choose an optimal waveguide dimension providing the lowest

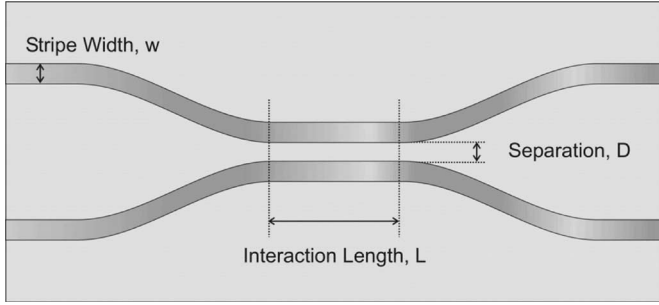


Fig. 6. Schematic of the directional coupler (DC) constructed straight waveguides and cosine-bends.

insertion (propagation and coupling) loss. One can also employ tapered-in width stripes, which independently minimizes the propagation and coupling losses.

### V. DIRECTIONAL COUPLERS: BASIC PROPERTIES

DCs investigated in this paper consisted of two 112- $\mu\text{m}$ -separated straight waveguides that approached each other by means of 2.5-mm-long cosine bends [21], and had a straight interaction region, where the waveguides were placed sufficiently close to each other so that the optical energy could be transferred from one waveguide to the other (Fig. 6). DCs were based on stripe waveguides of different widths  $w$  (from 2 to 8  $\mu\text{m}$ ) and had different lengths  $L$  of the interaction region and separation distances between waveguides in the interaction region (edge-to-edge distance  $D$ , from 0 to 8  $\mu\text{m}$ ).

For DCs with the interaction length changing from 0.1 to 1.5 mm with a 0.1 mm step, the transmission through the direct and coupled arm was measured at the wavelength of 1570 nm using a tuneable laser. The dependence of the normalized power through a direct and a coupled arm for each of the DCs on interaction length is presented in Fig. 7 for three different separation distances  $D$  between the waveguides.

In order to estimate the DC coupling length, theoretical analysis for coupled optical waveguides can be performed using coupled-mode theory, which gives simple analytical solutions for the mode-coupling process in a DC device [22], [23].

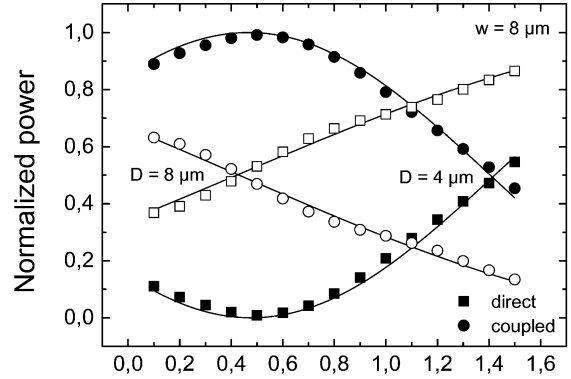
The power transmitted through the direct  $I_{\text{II}}$  and coupled  $I_x$  arms of a DC with the interaction length  $L$  can be written as [23]

$$I_{\text{II}} = \cos^2(\kappa L), \quad I_x = \sin^2(\kappa L) \quad (1)$$

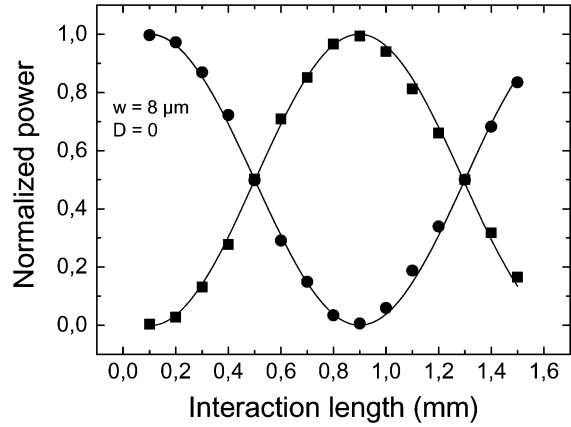
where  $\kappa$  is a wavelength-dependent coupling constant. The coupling length corresponding to full power transfer from one arm to another is then defined as

$$L_{\pi/2} = \frac{\pi}{2\kappa}. \quad (2)$$

The dependences of the transmitted power through one of the arms on the interaction length (Fig. 7) were fitted using (1) that allowed estimating the value of the coupling length and the offset, which gives a correction to the nominal interaction length owing to the interaction of the modes in the cosine-bend region [14]. For DCs based on 8- $\mu\text{m}$ -wide waveguides, the coupling length  $L_{\pi/2}$  was estimated to be around 0.8, 1.9, and 4.1 mm for the separation distances of 0, 4, and 8  $\mu\text{m}$ , respectively.



(a)



(b)

Fig. 7. Normalized power (power divided by the total power of two arms) through the direct and coupled arms versus the interaction length for DCs based on 8- $\mu\text{m}$ -wide ( $w$ ) waveguides. (a) 8- $\mu\text{m}$  (open symbols), 4- $\mu\text{m}$  (solid symbols) separation. (b) 0- $\mu\text{m}$  edge-to-edge separation ( $D$ ). Lines indicate the  $\sin^2$  and  $\cos^2$  fits [see (1)].

Dependences for DCs based on 4- $\mu\text{m}$ -wide stripes are shown in Fig. 8 for two different separation distances  $D$  between the waveguides. It is clear that in the case of narrow waveguide, full power transfer from one arm to another cannot be achieved. For zero-separated waveguides, a possible reason for the incomplete power transfer is that the coupling region consists of one 8- $\mu\text{m}$ -wide waveguide, so that the first higher order LR-SPP mode (the  $\text{asb}^0$  mode in the nomenclature of [10]) is most likely cutoff. In case of 4- $\mu\text{m}$ -separation, one can adapt the ideas developed for the four-port couplers [24] and suggest that the asymmetric super-mode supported by such couplers is most probably (or close to) cutoff. Thus, it cannot beat with the symmetric supermode [24, Fig. 15] to achieve synchronous coupling and hence complete power transfer. Weak confinement of the LR-SPP mode for relatively narrow stripes also influences coupler performance, since it results in the decrease of crosscoupling and increase of loss in the region of the cosine-bends (the cosine-bend used for the investigated DCs was designed to minimize the bend loss for a 8- $\mu\text{m}$ -wide waveguide).

We compared the experimentally obtained values of the coupling length with the modeling based on the effective-refractive-index approach [25], which was previously used for the configuration in question [15]. In this approach, the

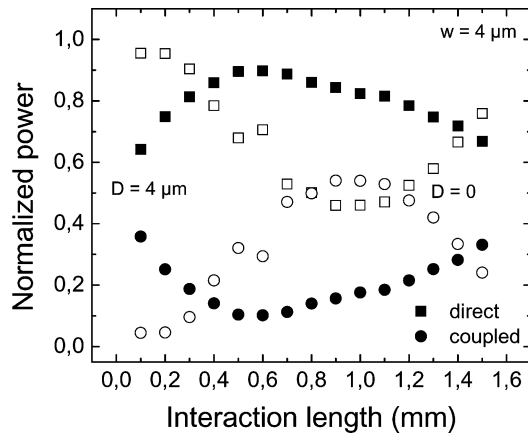


Fig. 8. Same as in Fig. 7 for DCs based on 4- $\mu\text{m}$ -wide waveguides with 4- $\mu\text{m}$  (solid symbols), 0- $\mu\text{m}$  (open symbols) separation.

TABLE I

COUPLING LENGTH AND OFFSET FOR DCs BASED ON 8- $\mu\text{m}$ -WIDE WAVEGUIDES WITH DIFFERENT SEPARATION DISTANCES. THEORETICAL VALUES ARE CALCULATED USING THE EFFECTIVE REFRACTIVE INDEX METHOD

Waveguide Separation, $\mu\text{m}$	Coupling Length, mm (experiment)	Coupling Length, mm (theory)	Offset, mm (experiment)
8	4.68	4.1	1.3
8	4.1	4.1	1.6
4	2.17	1.9	1.3
4	1.9	1.9	1.4
4	1.88	1.9	1.4
0	0.8	0.9	0.7

coupling length for a DC is obtained by calculating the beat length between the first two (lowest order) modes of the composite structure of two separated waveguides. For a 14-nm-thick and 16- $\mu\text{m}$ -wide waveguide, which corresponds to the DC based on 8- $\mu\text{m}$ -wide stripes with 0- $\mu\text{m}$ -separation, the beat length was calculated to be 0.91 mm, which is close to the experimentally obtained value of 0.8 mm (Table I). For the first two modes of the structure, consisting of two 8- $\mu\text{m}$ -wide waveguides with 4 and 8  $\mu\text{m}$  separation, the beat (coupling) length was found to be 1.9 and 4.1 mm, respectively, matching closely the experimental values (Table I). It should be noted that Table I contains the experimental results obtained with different samples, showing slightly different values of the coupling length. The observed variations are related to the circumstance that waveguide structures fabricated on different substrates might have slightly different parameters, such as thickness of the metal stripe and properties of the polymer claddings.

One interesting feature observed is that, at the nominal-zero-interaction length, the output power at the coupled arm was higher than that in the direct arm (Fig. 7). The length dependencies (Fig. 7) that were fitted using (1) allowed us to evaluate the offset, which gives a correction to the nominal interaction length due to the interaction of the modes in the  $S$ -bend region. This offset indicates that the interaction between two waveguides also occurs outside the parallel section. In the case of 4- $\mu\text{m}$ -separation between the waveguides, the offset value

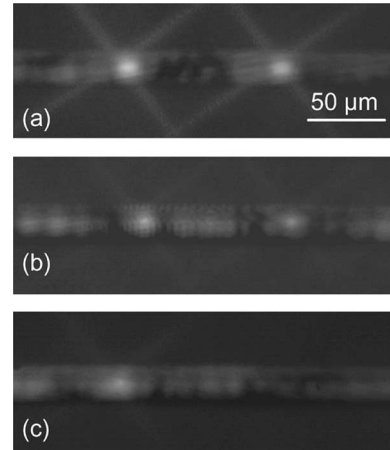


Fig. 9. DC output modes (direct arm to the left) for the waveguide widths. (a) 8  $\mu\text{m}$ . (b) 4  $\mu\text{m}$ . (c) 2  $\mu\text{m}$ . Waveguides are 0  $\mu\text{m}$  separated in the interaction region. The output arms separation is 104  $\mu\text{m}$ .

obtained from the fit was 1.4 mm, while for the 0- $\mu\text{m}$ -separated waveguides, this distance was about 0.7 mm (Table I). These offset values can be qualitatively accounted for by assuming that the (relatively efficient) interaction of the modes starts in the area of the cosine-bend, where the distance between the waveguide centers is approximately twice as large as that in the nominal interaction region. This effect was also noted in the couplers reported in [24]. Coupling along the  $S$ -bend region is very pronounced (Fig. 7) and has to be taken into account while designing the waveguide components containing DCs.

Examples of the output-intensity distribution observed for two DC arms are shown in Fig. 9 for DCs based on waveguides of different widths. The output modes for 8- $\mu\text{m}$ -wide waveguides demonstrated well-defined output modes from both arms and low level of background light in the polymer cladding. For narrow waveguides (2 and 4  $\mu\text{m}$  wide), the output modes were less defined compared to the background owing to weaker confinement of guided LR-SPP modes. Owing to weaker mode confinement in narrow waveguides as compared to wider waveguides, higher bend loss should be expected and was indeed observed for narrow LR-SPP waveguides.

## VI. DIRECTIONAL COUPLERS: WAVELENGTH SELECTION

The coupling length of a DC is determined by the difference in the propagation constants of even and odd combinations of individual modes and is, thereby, wavelength dependent. Thus, considering the practical applications, it is clear that the LR-SPP-based DCs with long interaction lengths can be used for wavelength division/multiplexing, i.e., as simple add-drop multiplexers. Typical transmission spectra for the direct and coupled arms of the DCs based on 8- $\mu\text{m}$ -wide waveguides with the interaction length of 8 mm are presented in Fig. 10 for three different separation distances. Transmission spectra are normalized to the straight stripe transmission of the same length as a DC, which demonstrates that the investigated DCs exhibit effectively lossless performance. Spectra were recorded in a very broad wavelength range from 950 to 1690 nm and showed

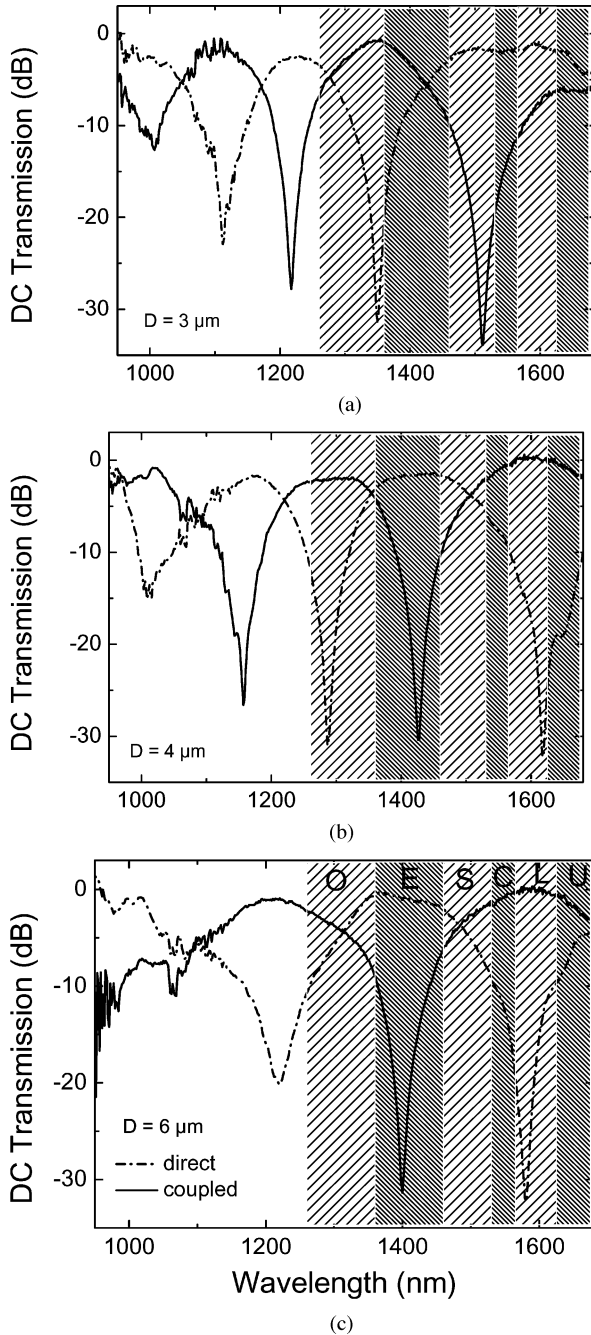


Fig. 10. Transmission through the direct and coupled arms of DCs based on 8- $\mu\text{m}$ -wide waveguides. (a) 3- $\mu\text{m}$  separation. (b) 4- $\mu\text{m}$  separation. (c) 6- $\mu\text{m}$  separation. Interaction length 8 mm.

efficient ( $\sim 30$  dB) power transfer from one arm to another dividing the signal between different telecom wavelength bands.<sup>2</sup>

The DC coupling length can also be estimated from the broadband transmission spectra. Applying the aforementioned mode

<sup>2</sup>Wavelength bands for telecommunication windows (2006). O-Original-band 1260 to 1360 nm; E-Extended-band 1360 to 1460 nm; S-Short wavelengths-band 1460 to 1530 nm; C-Conventional ("erbium window")-band 1530 to 1565 nm; L-Long wavelengths-band 1565 to 1625 nm; U-Ultralong wavelengths-band 1625 to 1675 nm. [Online]. Available: [http://www.nel-world.com/solutions/laser\\_diode.html](http://www.nel-world.com/solutions/laser_diode.html).

description to the investigated DCs, one can arrive at the simplified wavelength dependence of a coupling constant

$$\kappa = \frac{\pi \delta N}{\lambda} = \frac{q(w, D, \lambda)}{\lambda} \quad (3)$$

where  $\delta N$  is the effective index difference between the even and odd modes of the composite waveguide structure. This index difference (hence, the  $q$  parameter) depends on the waveguide parameters, separation distance as well as wavelength. The condition of complete separation (into two DC arms) of signals at two wavelengths gives

$$\frac{q(w, D, \lambda_1)L}{\lambda_1} - \frac{q(w, D, \lambda_2)L}{\lambda_2} = \frac{\pi}{2} \quad (4)$$

which corresponds to the distance between two nearest minima/maxima on the transmission spectra for the direct and coupled arms. For all spectra, two nearest minima were considered in the range from  $\sim 1400$  to 1600 nm separated by less than 190 nm giving the wavelength change of less than 13% in the region of interest. In this wavelength range, the variations in  $\delta N$  (calculated using the mode solver for wavelengths around 1400 and 1600 nm) are less than 17% allowing to neglect the wavelength dependence of  $\delta N$  in these approximate estimations. With these considerations in mind, the coupling constant can be roughly estimated as

$$\kappa = \frac{\pi \lambda_1 \lambda_2}{L \Delta \lambda} \frac{1}{\lambda}. \quad (5)$$

It should be mentioned that the interaction length  $L$  to be used in (4) and (5) should be corrected taking into account the offset values as discussed previously.

Using the procedure, coupling lengths for different separation distances were estimated from the DC transmission spectra. Coupling length values were found to change from 1.10 to 1.14 mm with the separation distance changing from 3 to 6  $\mu\text{m}$  that is of the same order of magnitude as the values obtained at 1570 nm. A relatively weak increase in the coupling length with the separation indicated that the mode description used throughout this paper is more appropriate than the often used weak-coupling approximation, in which an exponential increase in the coupling length is expected with the increase in waveguide separation [23].

Finally, we would like to outline the prospects for dynamic control of wavelength division/multiplexing with LR-SPP-based DCs that utilize the thermo-optic effect in the polymer cladding (the thermo-optic coefficient  $\partial n / \partial T \sim -2.5 \times 10^{-5} \text{ } ^\circ\text{C}^{-1}$  for BCB). The LR-SPP-based waveguide components provide a unique possibility of using the same metal-stripe circuitry for both guiding optical radiation and transmitting electrical signals that control its guidance. This fascinating feature has been recently demonstrated with the thermo-optic modulators and switches, including DCs, in which the effective index of LR-SPP modes of gold stripes was influenced by directly heating these stripes and, thereby, the surrounding polymer with electrical currents [15], [16]. It is relatively straightforward to extend this approach for the DCs considered in this section, so that the wavelength selection can be dynamically controlled. One can, for example, heat one of the two DC waveguides to

introduce a mismatch between the propagation constants of the individual LR-SPP waveguide modes [15]. As the coupling deteriorates owing to the thermally induced phase mismatch, it is expected that, depending on the interaction length and the applied power, one would be able to exchange the outputs for two different wavelengths or concentrating all the radiation in one output channel. In another approach, one can simultaneously heat both DC waveguides aiming at affecting their mode distributions rather than the propagation constants. It is known that, at relatively modest applied powers ( $\sim 15$  mW/mm for the BCB polymer), the LR-SPP waveguide approaches the cut-off value because the thermo-optic coefficient in polymers is negative [16]. This implies that the LR-SPP waveguide mode becomes very weakly localized—a circumstance that should strongly influence the coupling efficiency of a DC. The variation in the coupling constant would, in turn, change the wavelengths being spatially separated by the DC in accordance with (5). Finally, since the fact that the electrodes that can be used for heating are already in place, one can combine the aforementioned approaches to realize specific output states for the chosen wavelengths. Note that the switching power can be further decreased by using the polymers with larger thermo-optic effects. We believe that the above considerations clearly indicate that the dynamically controlled DCs represent a very attractive alternative for re-routing the optical signals in optical networks.

## VII. CONCLUSION

Guiding light along the thin metal stripes embedded in dielectric via excitation of long-range surface plasmon polaritons provides an alternative way of designing integrated optical circuits. LR-SPP-based technology offers low cost, easy fabrication, low propagation loss, efficient coupling with SM fibers, with flexibility and good performance. At telecom wavelength, the propagation loss of  $\sim 4$  dB/cm and coupling loss of the order of 2 dB have been obtained for a 14-nm-thick stripe waveguides of a few micrometers in width, implying that such components can be used as interconnections in the optical communication systems. As an example of applying the LR-SPP-based technology to economical and practical optical devices, directional couplers based on 8- $\mu\text{m}$ -wide stripe waveguides have been investigated. Coupling lengths of 4.1, 1.9, and 0.8 mm have been found for directional couplers with 8-, 4-, and 0- $\mu\text{m}$ -separated waveguides, respectively, implying that short (a few millimeters) and low-loss functional components (splitters, couplers, etc.) can be realized. Directional couplers have been modeled using the effective-refractive-index approach, and good agreement with the experimental results have been obtained. LR-SPP straight waveguides and directional couplers have been investigated in the wavelength range from 1000 to 1650 nm, showing acceptable loss levels and demonstrating the feasibility of LR-SPP-based components for operation in the very broad wavelength range. Demonstration of efficient routing of light using directional couplers based on LR-SPP stripe waveguides makes them promising candidates for novel-integrated optical components with high wavelength selectivity.

## ACKNOWLEDGMENT

The authors would like to thank K. Leosson for his help in fabricating the samples at Micro Managed Photons A/S.

## REFERENCES

- [1] H. Raether, *Surface Plasmons*. Berlin, Germany: Springer, 1988.
- [2] W. L. Barnes, A. Dereux, and T. W. Ebbesen, "Surface plasmon subwavelength optics," *Nature*, vol. 424, pp. 824–830, 2003.
- [3] I. I. Smolyaninov, D. L. Mazzoni, and C. C. Davis, "Imaging of surface plasmon scattering by lithographically created individual surface defects," *Phys. Rev. Lett.*, vol. 77, pp. 3877–3880, 1996.
- [4] S. I. Bozhevolnyi and F. A. Pudonin, "Two-dimensional micro-optics of surface plasmons," *Phys. Rev. Lett.*, vol. 78, pp. 2823–2826, 1997.
- [5] H. Ditlbacher, J. R. Krenn, G. Schider, A. Leitner, and F. R. Aussenegg, "Two-dimensional optics with surface plasmon polaritons," *Appl. Phys. Lett.*, vol. 81, pp. 1762–1764, 2002.
- [6] S. I. Bozhevolnyi, J. Erland, K. Leosson, P. M. W. Skovgaard, and J. M. Hvam, "Waveguiding in surface plasmon polariton band gap structures," *Phys. Rev. Lett.*, vol. 86, pp. 3008–3011, 2001.
- [7] S. I. Bozhevolnyi, V. S. Volkov, and K. Leosson, "Localization and waveguiding of surface plasmon polaritons in random nanostructures," *Phys. Rev. Lett.*, vol. 89, no. 18, p. 186801, 2002.
- [8] D. Sarid, "Long-range surface-plasma waves on very thin metal films," *Phys. Rev. Lett.*, vol. 47, pp. 1927–1930, 1981.
- [9] J. J. Burke, G. I. Stegeman, and T. Tamir, "Surface-polariton-like waves guided by thin, lossy metal films," *Phys. Rev. B, Condens. Matter*, vol. 33, pp. 5186–5201, 1986.
- [10] P. Berini, "Plasmon-polariton waves guided by thin lossy metal films of finite width: Bound modes of symmetric structures," *Phys. Rev. B, Condens. Matter*, vol. 61, pp. 10484–10503, 2000.
- [11] R. Charbonneau, P. Berini, E. Berolo, and E. Lisicka-Skrzek, "Experimental observation of plasmon-polariton waves supported by a thin metal film of finite width," *Opt. Lett.*, vol. 25, pp. 844–846, 2000.
- [12] T. Nikolajsen, K. Leosson, I. Salakhutdinov, and S. I. Bozhevolnyi, "Polymer-based surface-plasmon-polariton stripe waveguides at telecommunication wavelengths," *Appl. Phys. Lett.*, vol. 82, pp. 668–670, 2003.
- [13] P. Berini, R. Charbonneau, N. Lahoud, and G. Mattiussi, "Characterization of long-range surface-plasmon-polariton waveguides," *J. Appl. Phys.*, vol. 98, p. 043109, Aug. 2005.
- [14] R. Charbonneau, N. Lahoud, G. Mattiussi, and P. Berini, "Demonstration of integrated optics elements based on long-ranging surface plasmon polaritons," *Opt. Exp.*, vol. 13, pp. 977–984, 2005.
- [15] A. Boltasseva, T. Nikolajsen, K. Leosson, K. Kjaer, M. S. Larsen, and S. I. Bozhevolnyi, "Integrated optical components utilizing long-range surface plasmon polaritons," *J. Lightw. Technol.*, vol. 23, pp. 413–422, 2005.
- [16] T. Nikolajsen, K. Leosson, and S. I. Bozhevolnyi, "Surface plasmon polariton based modulators and switches operating at telecom wavelengths," *Appl. Phys. Lett.*, vol. 85, pp. 5833–5836, 2004.
- [17] T. Nikolajsen, K. Leosson, and S. I. Bozhevolnyi, "In-line extinction modulator based on long-range surface plasmon polaritons," *Opt. Commun.*, vol. 244, p. 455, 2005.
- [18] S. Jetté-Charbonneau, R. Charbonneau, N. Lahoud, G. Mattiussi, and P. Berini, "Demonstration of Bragg gratings based on long-ranging surface plasmon polariton waveguides," *Opt. Exp.*, vol. 13, pp. 4672–4682, 2005.
- [19] S. I. Bozhevolnyi, A. Boltasseva, T. Søndergaard, T. Nikolajsen, and K. Leosson, "Photonic band-gap structures for long-range surface plasmon polaritons," *Opt. Commun.*, vol. 250, pp. 328–333, 2005.
- [20] E. Palik, *Handbook of Optical Constants of Solids*. San Diego, CA: Academic, 1985.
- [21] A. Kumar and S. Aditya, "Performance of S-bends for integrated-optic waveguides," *Microw. Opt. Technol. Lett.*, vol. 19, pp. 289–292, 1998.
- [22] W.-P. Huang, "Coupled-mode theory for optical waveguides: An overview," *J. Opt. Soc. Am. A*, vol. 11, pp. 963–983, 1994.
- [23] N. S. Kapany and J. J. Burke, *Optical Waveguides*. New York: Academic, 1972.
- [24] R. Charbonneau, C. Scales, I. Breukelaar, S. Fafard, N. Lahoud, G. Mattiussi, and P. Berini, "Passive integrated optics elements based on long-range surface plasmon polaritons," *J. Lightw. Technol.*, no. 24, pp. 477–494, 2006.
- [25] H. Kogelnik, *Theory of Dielectric Waveguides*. Berlin, Germany: Springer, 1979, pp. 64–66.



**Alexandra Boltasseva** received the M.Sc. degree in physics from Moscow Institute of Physics and Technology, Moscow, Russia, in 2000, and the Ph.D. degree in electrical engineering from Technical University of Denmark (DTU), Lyngby, Denmark, in 2004.

She is currently a Postdoctoral Fellow at the Department of Communications, Optics and Materials, DTU after working with Micro Managed Photons A/S and Alight Technologies A/S. Her research focuses on surface-plasmon-polariton optics and advanced nanotechnology.



**Sergey I. Bozhevolnyi** received the M.Sc. degree in physics and the Ph.D. degree in quantum electronics, both from Moscow Institute of Physics and Technology, Moscow, Russia, in 1978 and 1981, respectively. He received the Dr.Sc. degree from Aarhus University, Aarhus, Denmark, in 1998.

From 1990 to 1991, he was with the Institute of Microelectronics, Russian Academy of Sciences, as the Head of Optical Technologies after working as an Associate Professor at the Yaroslavl Technical University, Yaroslavl, Russia, from 1981 to 1990. He

carried on research on near-field optics at the Institute of Physics, Aalborg University, Aalborg, Denmark, in 1991, where he has been a Professor, since 2003. His current research interests include linear and nonlinear nano-optics, surface plasmon polaritons and nano-plasmonic circuits, multiple light scattering including photonic band gap and light localization phenomena, and integrated fiber optics.